

AD-A038 398

CALIFORNIA UNIV LOS ANGELES DEPT OF MATERIALS

F/G 11/6

STRAIN ENERGY CONSIDERATION OF MARTENSITIC TRANSFORMATION IN TI--ETC(U)

MAR 77 M SHIBATA, K ONO

N00014-75-C-0889

UNCLASSIFIED

TR-3

NL

1 OF 1
AD
A038398



END
DATE
FILMED
5-77

ADA 038398

12

Technical Report No. 3

to the

Office of Naval Research

Contract No. N00014-75-C-0889

NR 031-781

STRAIN ENERGY CONSIDERATION OF MARTENSITIC
TRANSFORMATION IN TITANIUM ALLOYS

by

M. Shibata and Kanji Ono
MATERIALS DEPARTMENT
School of Engineering and Applied Science
University of California
Los Angeles, California 90024

March 1977

DDC
RECEIVED
APR 20 1977
A

DISTRIBUTION STATEMENT A
Approved for public release;
Distribution Unlimited

Reproduction in whole or in part is permitted for any
purpose of the United States Government.

ADJ NO. _____
DDC FILE COPY

REPORT DOCUMENTATION PAGE		READ INSTRUCTIONS BEFORE COMPLETING FORM
1. REPORT NUMBER ONR Technical Report # 3	7. GOVT ACCESSION NO.	3. REFERENCE CATALOG NUMBER
4. TITLE (and Subtitle) Strain Energy Consideration of Martensitic Transformation in Titanium Alloys		5. TYPE OF REPORT & PERIOD COVERED Technical rept.
7. AUTHOR(s) M. Shibata and Kanji Ono		6. PERFORMING ORG. REPORT NUMBER
9. PERFORMING ORGANIZATION NAME AND ADDRESS Materials Department, School of Engineering 6531-Boelter Hall, University of California Los Angeles, California 22217		8. CONTRACT OR GRANT NUMBER(s) N00014-75-C-0889 NR 031-781
11. CONTROLLING OFFICE NAME AND ADDRESS Metallurgy Program Office of Naval Research, 800 N. Quincy Street Arlington, Virginia 22217		10. PROGRAM ELEMENT, PROJECT, TASK AREA & WORK UNIT NUMBERS
14. MONITORING AGENCY NAME & ADDRESS (if different from Controlling Office) 24p. TR-3		12. REPORT DATE March 1977
		13. NUMBER OF PAGES 21
		15. SECURITY CLASS. (of this report) unclassified
		15a. DECLASSIFICATION/DOWNGRADING SCHEDULE
16. DISTRIBUTION STATEMENT (of this Report) Unlimited		
17. DISTRIBUTION STATEMENT (of the abstract entered in Block 20, if different from Report)		
18. SUPPLEMENTARY NOTES		
19. KEY WORDS (Continue on reverse side if necessary and identify by block number) Phase Transformation Strain Energy Titanium Alloys Plastic Relaxation Strain Martensite Habit Planes		
20. ABSTRACT (Continue on reverse side if necessary and identify by block number) See the following page		



ABSTRACT

Total strain energy of bcc to hcp martensitic transformation in several titanium alloys has been evaluated. Its minimum is assumed to dictate the characteristics of a transformation product and various features of Ti alloy martensites have been deduced. This analysis considered both elastic strain energy originated from the transformation strain and plastic relaxation strain in relief of high internal stresses. The primary mode of deformation evaluated for the latter was $\{10\bar{1}1\}\langle\bar{1}012\rangle$ twin. In Ti-Ta and Ti-Zr alloys, the usual $\{334\}_B$ habit was predicted for all the twin variants and the amount of twin shear was approximately 0.02. The results are similar to those reported for Ti martensite. In Ti-Cr and Ti-Mn alloys, both the $\{334\}_B$ and $\{344\}_B$ habits were found to be favorable, depending on the specific variant of twin shear, the amount of which was approximately 0.04. Theoretical predictions on the habit plane, shear mode and twin fraction are in good agreement with the experimental observations in the literature.



DISTRIBUTION STATEMENT NTIS <input type="checkbox"/> White Section DOC <input type="checkbox"/> Full Section UNANNOUNCED <input type="checkbox"/> JUSTIFICATION.....	
BY..... DISTRIBUTION AVAILABILITY CODE:	
Dist.	AVAIL. and/or SPECIAL
A	

1. INTRODUCTION

The importance of strain energy contribution to the free energy change during a phase transformation has been well established. However, the explicit evaluation is often cumbersome and only a limited number of calculations has been made. Over the years, such simplified cases as a spheroidal inclusion with hydrostatic transformation strain¹ have been employed as approximations. Recently, the Eshelby theory of the strain energy in a constrained transformation² has been invoked in the treatment of more generalized transformation strains involving martensitic transformations of Ti³, and steels^{4,5}. Other developments in this field include more elaborate theories for the evaluation of the strain energy of an ellipsoidal inclusion having non-uniformly distributed transformation strain in an anisotropic matrix^{6,7}, and the calculation of the strain energy in the reciprocal space⁸⁻¹⁰. The latter has been applied to studies of some phase transformation^{11,12}.

In our first paper³, we evaluated the strain energy due to the bcc to hcp phase transformation in titanium. The transformation strain, e_{ij}^t , was deduced from the Burgers' shear mechanism¹³, and the Eshelby theory² on the strain energy of ellipsoidal inclusion was employed. It was found that the strain energy is dependent on the orientation as well as on the aspect ratio of a spheroidal inclusion. The energy minima were found, when a disc-shaped inclusion was lying on $\{334\}_B$, which coincided with the habit plane of Ti martensite.

Subsequently, the calculation was extended to obtain the conditions that minimize total strain energy of transformation¹⁴. It was shown that even when the elastic strain energy is minimized, a large compressive stress component within the newly formed martensite phase exists. This internal stress can be reduced by uniform plastic deformation within the new phase. Denoting

plastic deformation or plastic relaxation strain (PRS) as e_{ij}^r , total stress-free or eigen strain, e_{ij}^* , becomes,

$$e_{ij}^* = e_{ij}^t + e_{ij}^r . \quad (1)$$

Now the elastic strain energy, E_s , is calculated by using e_{ij}^* , and the work done by the plastic deformation is added to evaluate the total strain energy, E , as

$$E = E_s (e_{ij}^*) + E_p (e_{ij}^r), \quad (2)$$

where the work done by the plastic relaxation strain, E_p , can be written as

$$E_p = V_I \cdot \tau_c \cdot \gamma . \quad (3)$$

Here V_I is the volume of a spheroidal inclusion, and τ_c and γ are the critical shear stress and the magnitude of simple shear of the PRS, respectively. The basic hypothesis of this modified approach can be stated as follows: *The condition of minimum strain energy dictates the morphology and orientation of a transformation product and the amount and type of plastic relaxation strain.*

The theory was applied to the study of martensitic transformation in pure Ti¹⁴. In order to reduce the elastic strain energy resulting from the phase change, a total of 84 glide and twin systems in the new phase was considered as PRS. It was found that for oblate spheroidal martensites with aspect ratios (thickness/diameter) less than 0.01, three types of PRS's; namely, $\{10\bar{1}1\}\langle\bar{1}012\rangle$ twin and $\langle a + c \rangle$ glides on $\{10\bar{1}1\}$ and $\{11\bar{2}2\}$, produce strain energy minima at shear strain of about 2%. Theoretical predictions on habit plane, shape shear, the amount and type of PRS, etc. were in excellent agreement with experimental

observations.

In this paper, we wish to apply this modified approach to the bcc to hcp martensitic transformation in Ti binary alloys. The experimental results of habit planes for hcp martensites have been reported to be $\{334\}_B$, $\{344\}_B$, or both $\{334\}_B$ and $\{344\}_B$. The most common was the $\{334\}_B$ habit observed in many dilute alloys^{15,16}. The $\{344\}_B$ habit was reported in Ti-Mn alloy¹⁷, but the mixed habit was also found in Ti-Mn¹⁸ and Ti-Mo¹⁹ alloys. Because of the availability of experimental observations, martensitic transformations of Ti-5.5Cr, -4.4Mn, -7.0Ta, and -12Zr alloys (alloying content given in atomic %) are selected here for the comparison with the predictions of the theory.

2. ELASTIC STRAIN ENERGY

Employing lattice parameter data of Ti binary alloys collected by Hansen et al.²⁰, e_{ij}^t for all the alloys were evaluated again assuming the Burgers' shear mechanism. The results are tabulated in Table I, where the reference coordinate axes are parallel to $[\bar{1}\bar{1}\bar{1}]_B$, $[2\bar{1}\bar{1}]_B$ and $[011]_B$, respectively. Note that $[011]_B$ is transformed to $[0001]_H$ by the Burgers' shear mechanism. Lattice parameters of α' phase in Ti-Mn and -Cr systems were assumed to be identical to those of pure Ti.

The main difference in components of e_{ij}^t among those alloys exists in e_{33}^t , which is the normal strain component along $[0001]_H$. In Ti-Mn and -Cr alloys, the magnitude of e_{33}^t is nearly twice that of pure Ti. In Ti-Zr and -Ta alloys, e_{ij}^t are very similar to that of pure Ti.

Consider next the plastic relaxation strain e_{ij}^r . In our previous analysis of pure Ti martensite, 84 possible shear systems were considered. It was found that the shear systems can be classified into four different types in terms of their effect on E_s . Two of them, Type I and II were found to lower E_s for thin plate morphologies. For the analyses of Ti alloy martensites, $\{10\bar{1}\}$

twin and basal glide were chosen to represent Type I and II, respectively. The first choice stems from the fact that it has been confirmed experimentally to be the primary martensite substructure in those alloys. The second is included for the sake of a comparison.

Now for a given variant of PRS in a given alloy, the total eigen strain e_{ij}^* was obtained in the reference coordinate system as a function of γ . In order to determine the orientation dependence of E_s , this eigen strain was transformed to that in another coordinate system, X_1' , X_2' and X_3' . These axes are parallel to the principal axes of an oblate spheroidal martensite. The transformed eigen strain, $e_{ij}^{*'}$ is given by

$$e_{ij}^{*'} = a_{ip} a_{jq} e_{pq}^* \quad (4)$$

where a_{ip} is the direction cosine between the reference coordinate axis X_p and the inclusion coordinate X_i' . The elastic strain energy of the oblate spheroidal inclusion can be found by the procedures described in reference 3. From a series of computer-aided calculations, it was possible to find the disc orientation, which gives the minimum elastic strain energy, E_{min} , as a function of γ and the aspect ratio, k , of the inclusion.

3. RESULTS OF CALCULATIONS

3.1 Elastic Strain Energy Minimum

When PRS of either Type I or II was included in e_{ij}^* , the minimum elastic strain energy, E_{min} , was reduced drastically. Figures 1 and 2 are the plots E_{min} vs. γ for $k = 0$ and $k = 0.01$, respectively. The dotted lines are the results for the Ti-Zr alloy. The Ti-Ta alloy behaves almost identically to the Ti-Zr alloy for an identical PRS, reflecting the similarity in e_{ij}^t . In these two alloys, the amount of shear required for minimizing E_{min} (defined as γ_c) was

approximately 0.02 for Type I and 0.08 for Type II, respectively. The solid lines in Figs. 1 and 2 show the corresponding variation in E_{\min} in the Ti-Mn alloy. Results for the Ti-Cr alloy were similar to those of the Ti-Mn alloy. In the Ti-Mn and -Cr alloys, the amount of shear needed to minimize E_{\min} increased to 0.04 for Type I and 0.10 for Type II. When $k = 0$, the values of E_{\min} were reduced to zero with the addition of PRS. The lowest value of E_{\min} increased with a higher aspect ratio. Numerical results are summarized in Table II. Note that even at $k > 0$, the minimum value of E_{\min} in the Ti-Mn alloy with Type I PRS is equal to that in pure Ti, which was reported in reference 14. On the other hand, the minimum value of E_{\min} with Type II PRS in Ti-Mn alloy is larger than that in pure Ti.

3.2 Total Strain Energy Minimum

While E_{\min} can be reduced by a substantial amount with the addition of PRS, this plastic relaxation strain also contributes to the total strain energy. Figure 3 and 4 are the plots of E vs. γ in the Ti-Mn alloy with $\{1011\}$ twin (Type I PRS) at $k = 0$ and $k = 0.01$, respectively. The critical shear stress, τ_c , in Eq. (3) for a given shear system is expressed as $\alpha \cdot \mu$ where μ is the shear modulus, and the values of α employed are shown in the figures. It is seen that, with Type I PRS, the total strain energy, E , reaches a minimum value (E^m) at $\gamma = \gamma_c$ even when α is as high as 0.01 (see Fig. 3). Similar results of E vs. γ were obtained with Type II PRS. In this case, however, the total strain energy was reduced only when α was less than 0.005. Numerical results of E^m and γ_c are given in Table III. In the Ti-Cr alloy, the relationships between E and γ were similar to those in the Ti-Mn alloy as described above. In the cases of the Ti-Zr and -Ta alloys, the relationships were close to those in pure Ti reported previously¹⁴.

4. DISCUSSION

The total strain energy being considered in our theory must be smaller than the magnitude of the chemical free energy change, $|\Delta F_c|$, in the phase transformation. Here, $|\Delta F_c|$ were evaluated by using Kaufman's formula for Ti binary alloys²¹. In all the alloys considered, it was found that $|\Delta F_c|$ is greater than E_{\min} for the inclusion with $k < 0.01$ even when PRS is ignored. Therefore, insofar as the energy balance is concerned, alloy martensites with the very thin disc morphology can exist without any plastic relaxation.

In order to reduce total strain energy via the operation of PRS, it is necessary that the resolved shear stress (RSS) on a particular shear system exceeds its critical shear stress (CSS) at the M_s temperature. The internal stress due to e_{ij}^t alone inside martensites in all the alloys considered was found to be essentially a large compressive stress along $[0001]_H$. Let us first consider $\{10\bar{1}1\}$ twin system (Type I PRS). The RSS on this twin system under the above mentioned condition can be easily found by using the transformation law for second-order Cartesian tensors. For $k = 0$, the RSS for $\{10\bar{1}1\}$ twin in a given alloy is given in Table IV. These values turned out to be almost independent of k . On the other hand, it is difficult to determine the effect of alloy addition on the CSS of $\{10\bar{1}1\}$ twin system in Ti alloys. We estimated this quantity from the plasticity data in polycrystalline Ti alloys at elevated temperatures and the CSS data in pure Ti^{22,23}. Table IV lists the calculated values of RSS and estimated values of CSS at M_s temperature²⁴. It is seen that in all the alloys, the RSS is much larger than the CSS. Thus, it is expected to observe this twin system in Ti alloy martensites in agreement with previous studies^{17,25,26,27}.

The observed twin fraction in Ti-4.4Mn martensite was reported to be 0.2 ~ 0.25¹⁷. Our prediction of the twin fraction is 0.28 ~ 0.29, when k is in

the range of 0 to 0.01 and α is taken as 0.005. This value of α corresponds to the estimated CSS. Theory and experiment agree well in this case. The average twin fraction observed in Ti-7.0Ta martensite was 0.10 ~ 0.15²⁵. This agrees reasonably well with our results. The predicted twin fraction was in the range of 0.17 ~ 0.20, corresponding to k of 0 to 0.01 and α of 0.002. According to the present calculation, martensite of the Ti-Cr alloy is expected to exhibit the same PRS as that of the Ti-Mn alloy. In Ti-Cr alloys, however, another type of twin, $\{10\bar{1}2\}\langle T011\rangle$, was reported in martensite in addition to the usual $\{10\bar{1}1\}$ twin²⁷. It is not clear why both twin systems coexist, since the shear directions are opposite.

The RSS of basal glide (Type II PRS) is zero for $k = 0$ and is always much smaller than that of $\{10\bar{1}1\}$ twin even for the cases of finite aspect ratios. Since Type II PRS is less effective in achieving the minimization of E_{\min} , the operation of this glide system is unlikely unless its CSS is considerably lower than that of Type I PRS. This appears not to be the case. Type II PRS was not reported in any of the microstructural studies^{17,26,28}.

Finally, predicted habit plane orientations are presented and compared with experimental observations. The plane normal to the minor axis of a thin oblate spheroidal inclusion is defined as the habit plane when the conditions of the elastic strain energy minimum were reached by using Eq. (4).

The habit plane orientations obtained without plastic relaxation strain were within several degrees of $[\bar{4}33]_B$. Those are indicated as P_0 in Fig. 5. In Ti-Ta and -Zr alloys, P_0 almost coincided with $[\bar{4}33]_B$ and also was essentially the same as that of pure Ti. In Ti-Mn and -Cr alloys, P_0 was shifted from $[\bar{4}33]_B$ toward $[\bar{1}11]_B$ by 3 to 4 degrees. The addition of plastic relaxation strain shifts the habit plane orientation from P_0 away from the 001 ~ 111 symmetry line. The predicted orientation corresponding to the total strain energy minimum depended on material (through e_{ij}^t and α) and also on the variant

of operating $\{10\bar{1}\}$ twin. It is interesting to note that the magnitude of L^m was unchanged even though different habit orientations resulted with different variants of $\{10\bar{1}\}$ twin system. In Ti-Ta and -Zr alloys, $\{10\bar{1}\}$ twin as PRS always resulted in the $\{334\}_B$ habit. Results for Ti-Ta alloy are shown in Fig. 5a (corresponding to E^m at $\alpha = 0$, $k = 0$). Six different habit orientations resulted from the six variants of this twin system are indicated in the figure. If $\alpha > 0$, E^m was achieved at a smaller amount of γ and the orientations predicted were closer to P_0 than the ones in Fig. 5a. Effects of k were small, as the predictions did not change more than 1 degree from the above results with $k = 0$ at a given α . Therefore, all the possible predictions in Ti-Ta and -Zr alloys happened to be the $\{334\}_B$ habit plane, as was the case in pure Ti¹⁴. No experimental determination of habit plane in these alloys is available for comparison, however.

In Ti-Mn and -Cr alloys, two out of the six variants of $\{10\bar{1}\}$ twin also produced basically the $[\bar{4}33]_B$ habit. In Fig. 5b, the results for Ti-Mn alloy are shown. Two of the six twin variants produced the habit orientations within a few degrees of $[\bar{4}43]_B$. The other two habit orientations were close to $[\bar{4}34]_B$. The specific K_1 planes of these variants are indicated in Fig. 5. These four orientations can be classified as the $\{344\}_B$ habit. These were determined at the total strain energy minima with $\alpha = 0$ and $k = 0$. As mentioned previously, k hardly affected the habit plane orientation, but effect of α was significant. When α was increased to 0.005, shifts in the habit orientations toward P_0 was observed as shown in Fig. 5c. Two variants of $\{10\bar{1}\}$ twin still produced the $\{344\}_B$ habit. Results for Ti-Cr alloy were essentially identical. Thus in these alloys, two groups of habit orientations are anticipated; one is close to the $\{334\}_B$ habit and the other, the $\{344\}_B$ habit. This is in agreement with an experimental finding in Ti-Mn alloys. Liu and Margolin reported these two habits in alloys containing 4.35 to 5.25 wt.Mn¹⁸. However, in Ti-Cr alloys,

only $\{334\}_B$ habit was reported experimentally^{15,27} in disagreement with the above prediction. In this alloy, a second type of twin, $\{10\bar{1}2\}\langle\bar{1}011\rangle$, was also observed in the martensite²⁷. The origin of the second shear is not known, but our calculations suggest that lowering of the strain energy is unlikely to be the reason.

5. REFERENCES

1. F.R.N. Nabarro: Proc. Roy. Soc., 1940, Vol. A175, p. 519.
2. J. D. Eshelby: Proc. Roy. Soc., 1957, Vol. A241, p. 376.
3. M. Shibata and K. Ono: Acta Met., 1975, Vol. 23, p. 587.
4. K. E. Easterling and A. R. Thörlén: Acta Met., 1976, Vol. 24, p. 333.
5. D. R. Clarke: Met. Trans., 1976, Vol. 7A, p. 723.
6. R. J. Asaro and D. M. Barnett: J. Mech. Phys. Solids, 1975, Vol. 23, p. 77.
7. T. Mura, T. Mori and M. Kato: J. Mech. Phys. Solids, 1976, Vol. 24, p. 305.
8. A. G. Khachaturyan: Sov. Phys. Solid St., 1967, Vol. 8, p. 2163.
9. A. G. Khachaturyan and V. N. Hairapetyan: Phys. Stat. Sol. (b), 1973, Vol. 57, p. 801.
10. H. Cook and D. deFontaine: Acta Met., 1969, Vol. 17, p. 915; 1970, Vol. 18, p. 189.
11. A. G. Khachaturyan and G. A. Shatalov: Sov. Phys. JETP, 1969, Vol. 29, p. 557.
12. J. A. Wert: Acta Met., 1976, Vol. 24, p. 65.
13. W. G. Burgers: Physica, 1934, Vol. 1, p. 561.
14. M. Shibata and K. Ono: Acta Met., 1977, Vol. 25, p. 35.
15. Y. C. Liu: Trans. AIME, 1956, Vol. 206, p. 1036.
16. W. K. Armitage: Physical Properties of Martensite and Bainite, Iron and Steel Institute Report #93, p. 76, London, 1965.
17. C. Hammond and P. M. Kelly: Acta Met., 1969, Vol. 17, p. 869.
18. Y. C. Liu and H. Margolin: Trans. AIME, 1953, Vol. 197, p. 667.
19. P. Gaunt and J. W. Christian: Acta Met., 1959, Vol. 7, p. 534.
20. M. Hansen, D. J. McPherson and W. Rostoker: Constitution of Titanium Alloy System, WADC Tech. Report 53-41, Wright Air Development Center, 1953.
21. L. Kaufman: Acta Met., 1959, Vol. 7, p. 575.
22. For example; H. K. Adenstedt: Handbook on Titanium, WADC Tech. Report 54-305, Part 1, Wright Air Development Center, 1954.

23. N. E. Paton and W. A. Backofen: *Met. Trans.*, 1970, Vol. 1, p. 2839.
24. P. Duwez: *Trans. ASM*, 1953, Vol. 45, p. 934.
25. K. A. Bywater and J. W. Christian: *Phil. Mag.*, 1972, Vol. 25, P. 1249.
26. S. Banerjee, S. J. Vijayakar, and R. Krishanan: *Titanium Science and Technology*, Vol. 3, p. 1597, Plenum, 1973.
27. R. H. Ericksen, R. Taggart and D. H. Polonis: *Acta Met.*, 1969, Vol. 17, p. 553.
28. J. C. Williams: *Titanium Science and Technology*, Vol. 3, p. 1433, Plenum, 1973.

TABLE I. Transformation Strain e_{ij}^t of Ti and its Alloys

Alloy	e_{11}^t	e_{12}^t	e_{13}^t	e_{22}^t	e_{23}^t	e_{33}^t
Ti-4.4 Mn	0.04535	-0.08839	0	-0.03978	0	0.01591
-5.5 Cr	0.04454	-0.08839	0	-0.04053	0	0.01512
-12 Zr	0.03912	-0.08839	0	-0.04551	0	0.00877
-7.0 Ta	0.03542	-0.08839	0	-0.04891	0	0.00765
pure Ti	0.03808	-0.08839	0	-0.04647	0	0.00884

Alloy	Aspect ratio	(011)[0112] Twin		(0001)[2110] Glide	
		$E_{min}/\mu V$	γ_c	$E_{min}/\mu V$	γ_c
Ti-4.4% Mn	0	0	0.038	0	0.11
	0.01	3.5×10^{-4}	0.042	4.7×10^{-4}	0.095
Ti-5.5% Cr	0	0	0.04	0	0.11
	0.01	3.5×10^{-4}	0.04	4.7×10^{-4}	0.09
Ti-12% Zr	0	0	0.02	0	0.08
	0.01	3.5×10^{-4}	0.02	4.2×10^{-4}	0.06
Ti-7.0% Ta	0	0	0.02	0	0.07
	0.01	3.5×10^{-4}	0.02	4.1×10^{-4}	0.06
pure Ti	0	0	0.02	0	0.08
	0.01	3.5×10^{-4}	0.02	4.1×10^{-4}	0.07

TABLE II. Minimum values of E_{min} and corresponding amounts of PRS required to achieve the strain energy minimization, γ_c .

P R S			k = 0		k = 0.01	
Type	Shear System	α	$E^m/\mu V_I$	γ_c	$E^m/\mu V_I$	γ_c
I	{10T1} Twin	0	0	0.038	3.4×10^{-4}	0.042
		0.001	3.8×10^{-5}	0.037	3.8×10^{-4}	0.040
		0.005	1.7×10^{-4}	0.028	5.2×10^{-4}	0.029
		0.01	2.7×10^{-4}	0.016	6.4×10^{-4}	0.017
II	Basal Glide	0	0	0.11	4.7×10^{-4}	0.095
		0.001	1.0×10^{-4}	0.10	5.6×10^{-4}	0.085

TABLE III. E^m and γ_c in the Ti-4.4Mn Alloy.

Alloy	R S S		Estimated CSS at M_s	
	τ	α	τ_c	α
	MPa		MPa	
Ti-4.4 Mn	687	0.0178	157~470	0.0041~0.0122
-5.5 Cr	627	0.0169	124~353	0.0034~0.0095
-12 Zr	304	0.0098	71	0.0023
-7.0 Ta	284	0.0086	74	0.0023
Pure Ti	294	0.0099	50	0.0017

Table IV. Resolved Shear Stress (RSS) due to Transformation Strain and Estimated Critical Shear Stress (CSS) of $\{10\bar{1}1\}\langle 1012\rangle$ Twin in Ti Alloy Martensites.

FIGURE CAPTION

Fig. 1: E_{\min} vs. γ in Ti-4.4Mn and -12Zr alloys ($k = 0$).

Fig. 2: E_{\min} vs. γ in Ti-4.4Mn and -12Zr alloys ($k = 0.01$).

Fig. 3: $(E_{\min} + E_p)$ vs. γ with $(01\bar{1}1)$ twin as PRS in Ti-4.4Mn alloy ($k = 0$).

Fig. 4: $(E_{\min} + E_p)$ vs. γ with $(01\bar{1}1)$ twin as PRS in Ti-4.4Mn alloy ($k = 0.01$).

Fig. 5: The orientation of predicted habit planes with six variants of $\{10\bar{1}1\}$

$\langle 1012 \rangle$ twin as PRS and $k = 0$

a) Ti-7.0 Ta alloy ($\alpha = 0$)

b) Ti-4.4Mn alloy ($\alpha = 0$)

c) Ti-4.4Mn alloy ($\alpha = 0.005$)

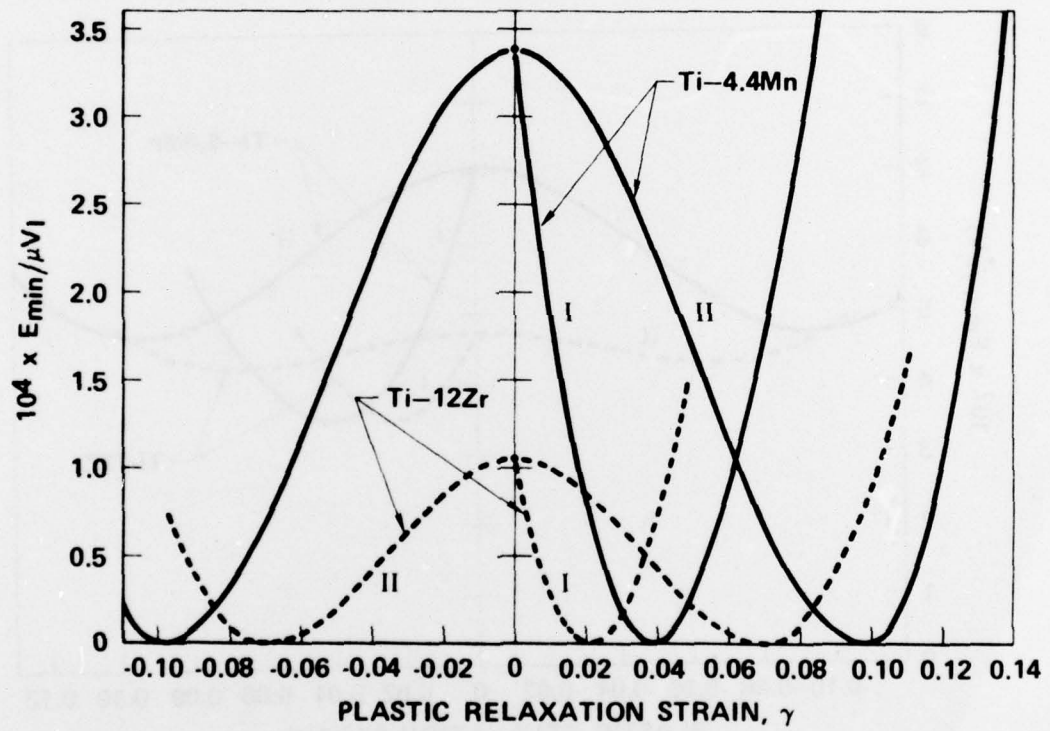


Figure 1

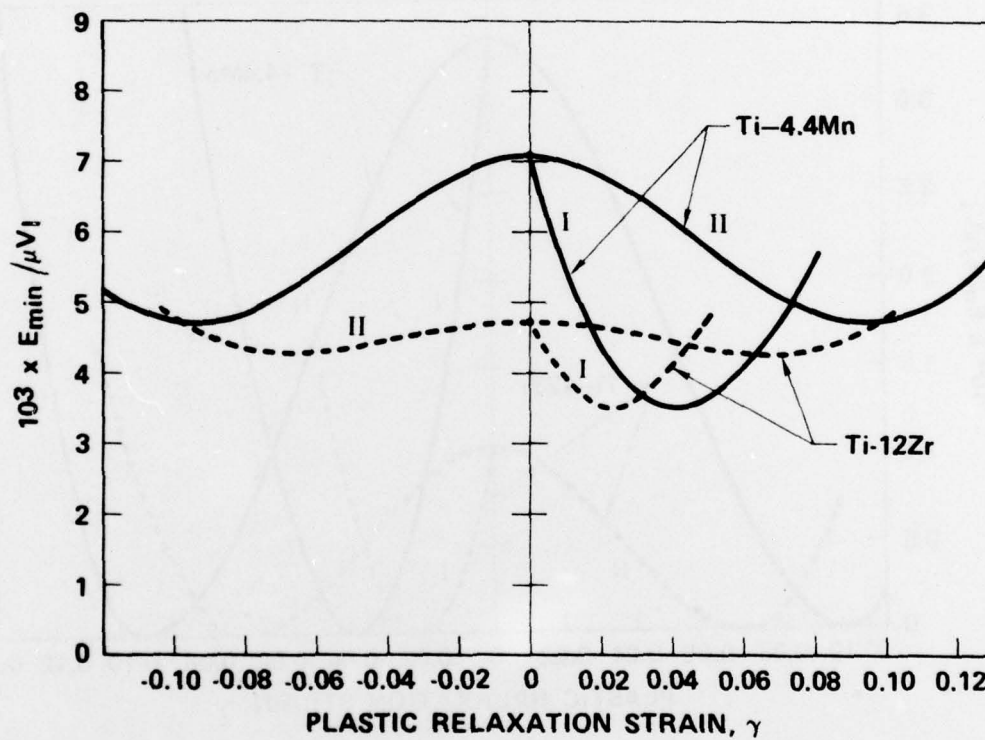


Figure 2

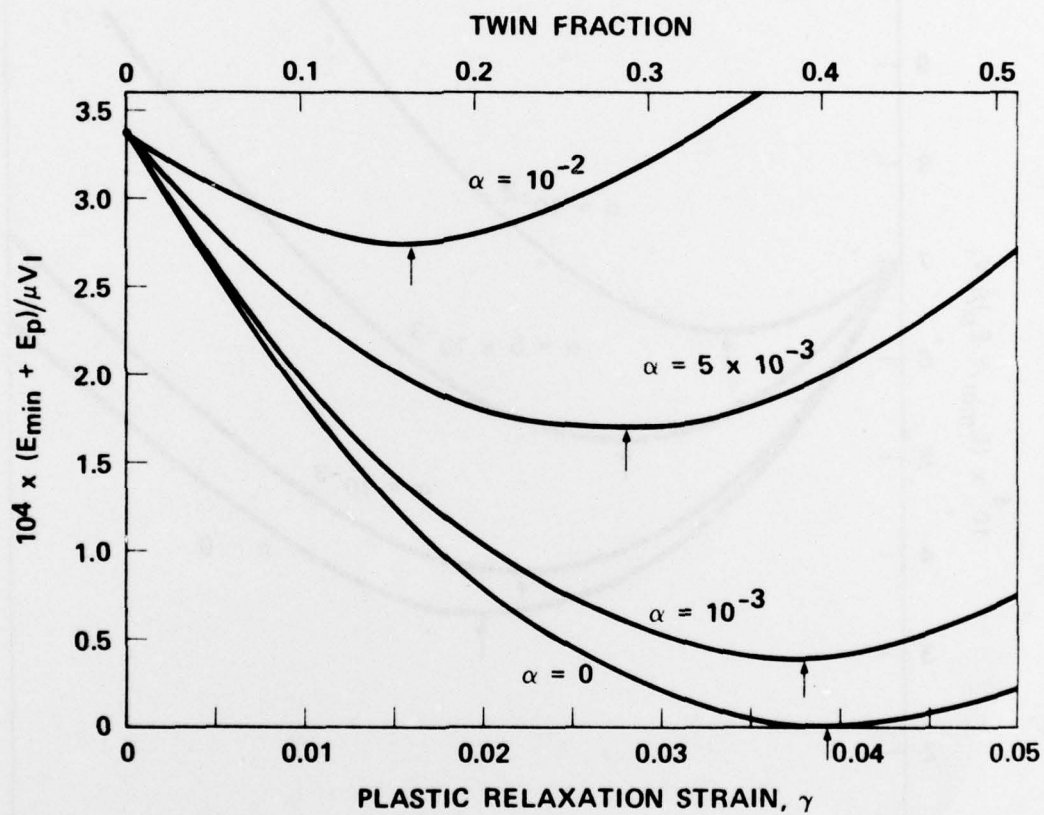


Figure 3

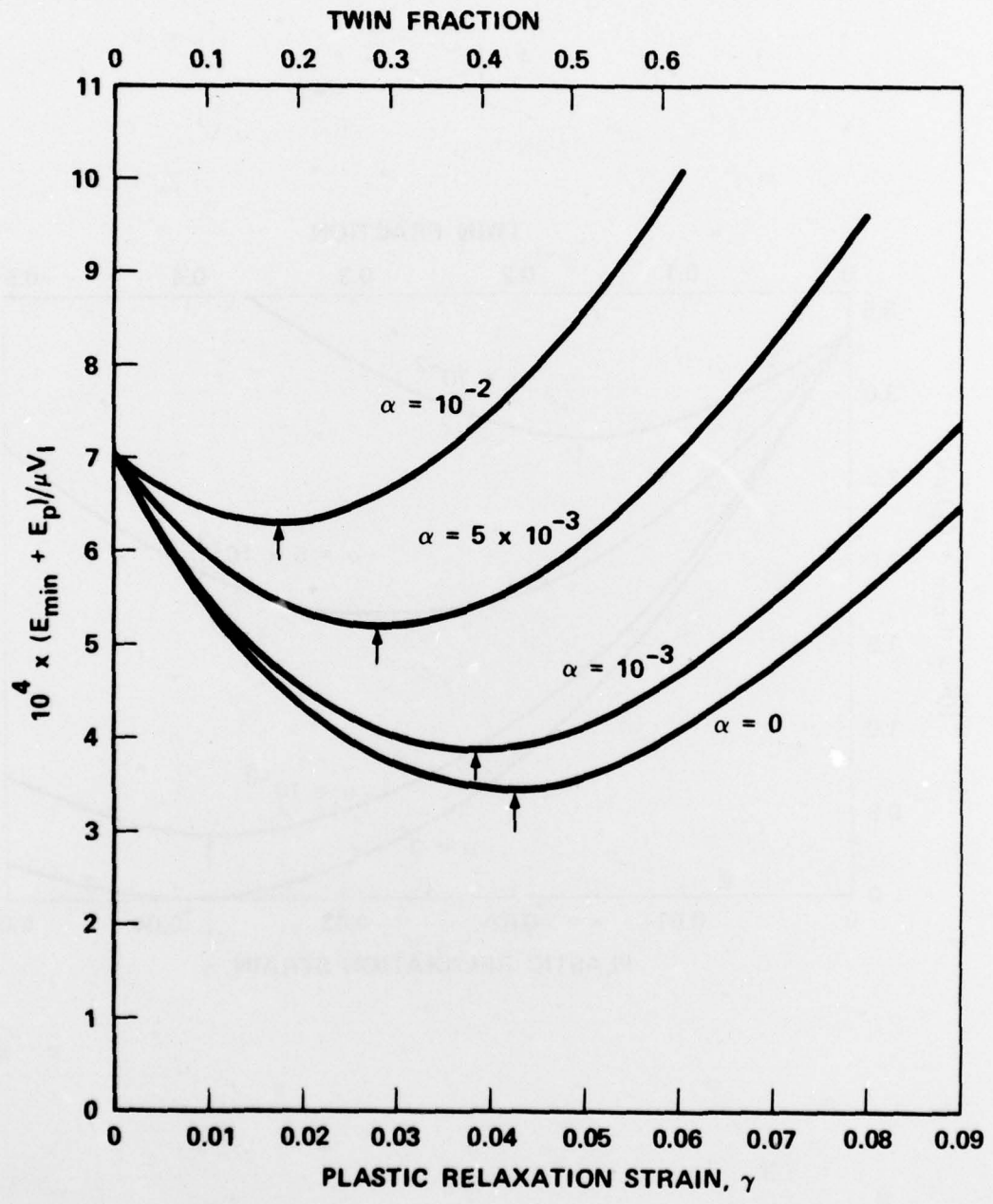
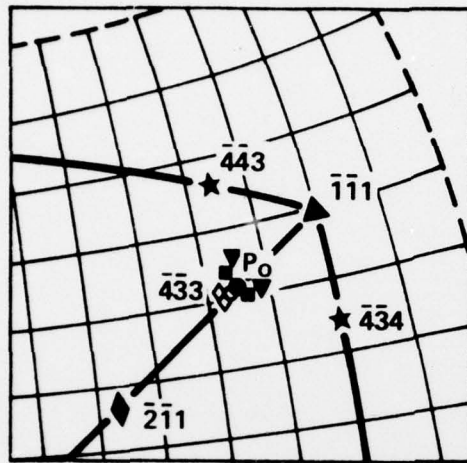
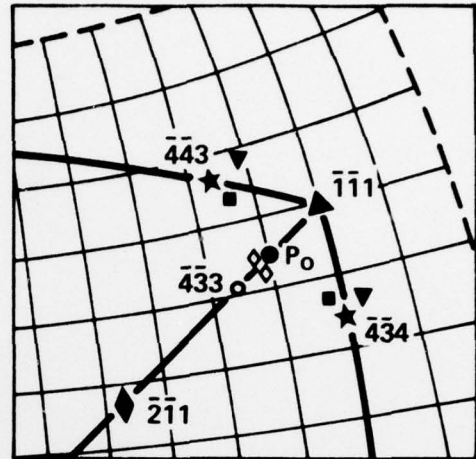


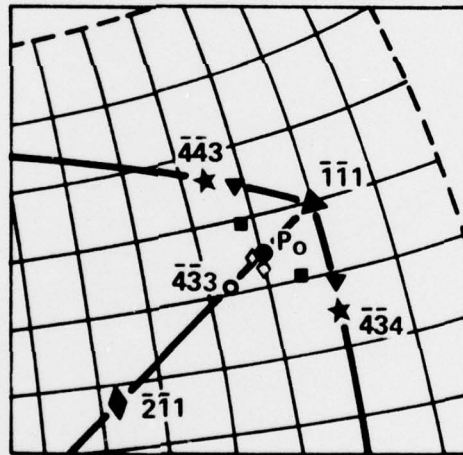
Figure 4



(a) Ti - 7.0 Ta at $\alpha = 0$



(b) Ti - 4.4 Mn at $\alpha = 0$



(c) Ti - 4.4 Mn at $\alpha = 0.005$

HABIT PLANE	VARIANT OF K_1 PLANE IN $\{10\bar{1}1\} \langle \bar{1}012 \rangle$ TWIN	
◇	$(1\bar{1}01)$, $(\bar{1}101)$
■	$(10\bar{1}1)$, $(\bar{1}011)$
▼	$(01\bar{1}1)$, $(0\bar{1}11)$

Figure 5